

Fast sound in liquid water

Umberto Balucani

Istituto di Elettronica Quantistica, Consiglio Nazionale delle Ricerche, 50127 Firenze, Italy

Giancarlo Ruocco

Dipartimento di Fisica dell'Università, 68100 L'Aquila, Italy

Alessandro Torcini

Dipartimento di Fisica dell'Università, 50125 Firenze, Italy

Renzo Vallauri

Dipartimento di Fisica dell'Università di Trento, 38050 Povo, Italy

(Received 10 August 1992)

Both inelastic-neutron-scattering experiments and computer simulations have established that liquid water can support a longitudinal mode propagating with a velocity much larger than the ordinary speed of sound. The physics behind this peculiar behavior is studied by a comprehensive microscopic approach. The effect is found to be a rather extreme case of a well-known phenomenon occurring even in monatomic liquids. To make the analogies and the differences more transparent, simulation data in water and in a simple alkali metal (liquid Cs near melting) are also reported. Finally, we discuss the ultimate microscopic origin of fast-sound effect in liquid water.

PACS number(s): 61.20.Lc, 61.25.Em, 61.20.Ja

I. INTRODUCTION

The occurrence of strongly directional intermolecular correlations (“hydrogen bonds”) is believed to be largely responsible for many unusual properties of water at the thermodynamic and structural level. These peculiarities have a counterpart in many time-dependent features and are expected to be particularly evident in those short-time (or high-frequency) properties which are dominantly associated with the hydrogen dynamics.

It is somehow more surprising to find that substantial “anomalies” in the dynamics are present even at the center-of-mass level. In the present work we shall explicitly consider the dynamics of density fluctuations of the centers of mass in liquid water. The peculiarities occur just outside the ordinary hydrodynamic regime, namely, for wave vectors k of some 10^7 cm^{-1} . In this range, inelastic-neutron-scattering data have been reported for heavy water at room temperature [1]. The presence of well-defined propagating “modes” at these k becomes questionable because of their strongly damped character, and a better insight into the underlying dynamics is provided by looking at longitudinal density currents. As a matter of fact, the neutron spectra do not show any apparent inelastic peak at the explored wave vectors; however, striking results are obtained in the analysis of the frequency “tails” (a procedure basically equivalent to the consideration of the longitudinal current spectra). More precisely, the analysis of the neutron data at the various wave vectors still yields an approximately linear dispersion law as in the hydrodynamic regime, but the associated “sound” velocity is found to be *more than twice* higher than the ordinary sound speed. This experimental result is consistent with the findings of a previous simulation

study [2].

Apparently, this unexpected feature has no quantitative parallel in the corresponding situation met in simple liquids, and this circumstance led to the speculation [1] that together with the “slow” sound ruled by the ordinary hydrodynamic laws, some specific mechanism typical of water may give rise to the *additional* presence of this fast sound.

On the other hand, the existence of a second sound mode has been cast in doubt by Wojcik and Clementi [3] on the basis of further simulation results obtained with an intermolecular potential model (usually referred to as MCY from the names of the proponents Matsuoka, Clementi, and Yoshimine) different from the one of Ref. [2]. The analysis of these data confirmed the existence and the magnitude of the fast-sound anomaly; however, no evidence of the *simultaneous* presence of two sound modes was found. As a consequence of these results, in Ref. [3] a possible alternative explanation of the anomaly was proposed in terms of a generalized hydrodynamical picture.

More recently, another computer experiment was performed in room-temperature water, modeled in terms of the transferable interaction potential with four points (TIP4P) intermolecular potential [4]. The data indicated the absence of two separate acoustic modes, thus confirming the findings of Ref. [3]. Moreover, additional pieces of information were provided by considering both the oxygen and the hydrogen density fluctuations. In particular, the latter (claimed in Ref. [2] to be directly associated with fast sound) were indeed found to support a collective high-frequency mode. However, rather than soundlike the dispersion of this mode has a clear “optical” character, with frequencies ω higher than 150 ps^{-1} at small wave vectors. These values are typical of libra-

tional modes, and are at least a factor 4 larger than the frequencies explored in Ref. [1]. On the other hand, over the ω range probed by the neutron experiment the hydrogen density spectra were found to be *identical* with those associated with oxygen atoms and/or with the molecular centers of mass. Qualitatively, these simulation findings are accounted for by an approximate Mori-Zwanzig analysis of the density fluctuations of the two species, expressed in terms of a two-component variable.

While ruling out any direct connection between the fast-sound anomaly and the hydrogen dynamics, the findings of Refs. [3,4] pave the way for a comprehensive microscopic interpretation of the peculiarity. This is the main purpose of the present work; as we shall see, the final result is that in this respect water does not need an approach *qualitatively* different from the one adopted in simple monatomic liquids. Albeit somehow less spectacular than the original speculation of Ref. [1], this “conventional” interpretation clarifies on a consistent physical basis the role of the quantities really relevant in the problem, as well as their microscopic origin. Within this framework and on a purely *quantitative* basis, we shall find that water indeed exhibits some unusual features when compared with typical simple liquids and that this circumstance is ultimately responsible for the “surprising” magnitude of the anomalous propagation effect.

The present paper is organized as follows. In Sec. II we review the basic concepts underlying the dynamics of density fluctuations in a monatomic liquid; to make a closer contact with a specific system, we shall report several results obtained in a recent computer simulation of liquid cesium near the melting point. The framework is subsequently applied to liquid water (Sec. III); in particular, in this system it is shown how such a rephrasing may yield results quantitatively different from the ones typical of simple liquids. Finally, in Sec. IV the ultimate origin of such a behavior is related to the microscopic structural properties of water.

II. DYNAMICS OF DENSITY FLUCTUATIONS IN MONATOMIC SYSTEMS

Before embarking on a discussion of the peculiarities of water, it is worthwhile to recall the approaches usually employed to investigate the dynamics of density and current fluctuations in a “simple” monatomic fluid. This offers the opportunity to discuss some typical results obtained in these systems by means of well-defined approximations, such as the viscoelastic model.

In a monatomic fluid characterized by N classical particles of mass M enclosed in a volume V and interacting through a pair potential $v(r)$, the dynamics of density fluctuations around the average value $n = N/V$ depends on the length scale actually sampled, i.e., on the associated wave vector \mathbf{k} . Denoting by $\mathbf{r}_j(t)$ the position of the j th particle at time t and introducing \mathbf{k} -dependent density fluctuations $\tilde{n}(\mathbf{k}, t) = \sum_j \exp[i\mathbf{k} \cdot \mathbf{r}_j(t)] - 8\pi^3 n \delta(\mathbf{k})$, the main dynamical quantity of interest is the intermediate scattering function $F(k, t) = \langle \tilde{n}^*(\mathbf{k}, 0) \tilde{n}(\mathbf{k}, t) \rangle$ along with its Fourier transform, the dynamic structure factor $S(k, \omega)$. With these definitions, the initial value $F(k, 0)$

coincides with the static structure factor $S(k)$. The Mori-Zwanzig formalism provides the following exact representation of the Laplace transform of $F(k, t)$:

$$F(k, s)/S(k) = \{s + \langle \omega_k^2 \rangle / [s + M(k, s)]\}^{-1}. \quad (1)$$

If $F(k, s)$ is known, the dynamic structure factor follows from $S(k, \omega) = (1/\pi) \text{Re} F(k, s = i\omega)$. In Eq. (1), $\langle \omega_k^2 \rangle = [k_B T / MS(k)] k^2$, where T is the temperature of the system; clearly, as $k \rightarrow 0$ $\langle \omega_k^2 \rangle \rightarrow c_T^2 k^2$, where c_T is the isothermal sound velocity. Finally, $M(k, s)$ is the Laplace transform of a memory function $M(k, t)$, a quantity which in a sense probes the dynamics at a more microscopic level than $F(k, t)$ itself. The exact details of this k -dependent dynamics are unknown, but the initial value reads $M(k, t = 0) \equiv \Delta_k = \omega_L^2(k) - \langle \omega_k^2 \rangle$, where [5]

$$\omega_L^2(k) = 3[k_B T / M] k^2 + \Omega_0^2 - \Omega_k^2 \quad (2)$$

and

$$\Omega_k^2 = (n/M) \int d\mathbf{r} \frac{\partial^2 v(r)}{\partial z^2} \exp(ikz) g(r). \quad (3)$$

Here $g(r)$ is the pair distribution function, and the external wave vector \mathbf{k} has been taken along the z axis. In simple liquids one may approximately write [6]

$$\omega_L^2(k) \approx 3[k_B T / M] k^2 + \Omega_0^2 [1 - j_0(kR) + 2j_2(kR)], \quad (4)$$

where the length R is of the order of σ , the minimum separation where $v(r) = 0$. The first “kinetic” term on the right-hand side is usually negligible, except at high wave vectors where the free-particle aspects take over. Thus the dominant contribution is provided by the term proportional to

$$\Omega_0^2 = (4\pi n / 3M) \int_0^\infty dr r^2 \{v''(r) + 2[v'(r)/r]\} g(r). \quad (5)$$

In a simple liquid, the inverse of the “Einstein frequency” Ω_0 is a measure of the time scale associated with the “rattling” motion of an atom in the cage of its neighbors. Typically, the potential $v(r)$ comprises both an attractive and a repulsive part, modeled as being, respectively, proportional to r^{-p} and r^{-q} with $p < q$. With this schematization, in simple liquids the quantity Ω_0^2 is approximately proportional to pq [5,7]. Thus a softer potential implies a smaller value of the Einstein frequency. Letting $R \approx \sigma$, for small k one finds

$$\omega_L^2(k \rightarrow 0) \equiv c_\infty^2 k^2 \approx 3[(k_B T / M) + (\Omega_0^2 \sigma^2 / 10)] k^2, \quad (6)$$

where the physical meaning of the “velocity” c_∞ will be clarified later on. Note that

$$(c_\infty / c_T)^2 \approx \frac{3}{10} S(0) \Gamma, \quad (7)$$

where the dimensionless parameter $\Gamma = M \Omega_0^2 \sigma^2 / k_B T$ is a measure of the relative importance of potential versus kinetic energy contributions.

A simple approximation for the time dependence of $M(k, t)$ is provided by the “viscoelastic” model [5,6]

$$M(k, t) = \Delta_k \exp(-t/\tau_k). \quad (8)$$

Equation (8) accounts for the elastic (solidlike) properties

of the system at short times (lumped in the quantity Δ_k), as well as for its overall liquidlike response at low frequencies [embodied in the quantity $M(k, z=0) = \Delta_k \tau_k$, essentially a wave-vector-dependent longitudinal viscosity coefficient]. Note that for $k \rightarrow 0$ the simple ansatz (8) does not take into proper account the presence of temperature fluctuations. In the Brillouin peak, the latter are responsible for the “renormalization” of the velocity of sound from its isothermal to the correct adiabatic value. The ansatz (8) can easily be improved in this respect, but this is hardly necessary in liquids having a ratio of the specific heats ≈ 1 (liquid alkali metals, water), in which the role of temperature fluctuations is virtually negligible.

The consequences of the viscoelastic model (8) on the dynamic structure factor follow straightforwardly from Eq. (1). In particular, comparing for $k \rightarrow 0$ this “viscoelastic” $S(k, \omega)$ with the correct hydrodynamic result under isothermal conditions, the quantity $\Delta_k \tau_k$ can be identified with the damping of the sound mode, yielding

$$(\tau_{k \rightarrow 0})^{-1} = nM \frac{c_\infty^2 - c_T^2}{\frac{4}{3}\eta + \eta_B}, \quad (9)$$

where η and η_B are the shear and the bulk viscosity coefficients, respectively. Since c_∞ is always found to be larger than c_T , the time $\tau_{k \rightarrow 0} \equiv \tau_0$ is found to be perfectly defined and finite in this $k \rightarrow 0$ limit. Even beyond the hydrodynamic regime, $S(k, \omega)$ may show two inelastic peaks, symmetrical around $\omega = 0$ and located at [6]

$$(\omega_k^2)_{\text{peak}} = \frac{1}{3} \{ \omega_L^4(k) - 2(1/\tau_k)^2 [2\omega_L^2(k) - 3\langle \omega_k^2 \rangle] + (1/\tau_k)^4 \}^{1/2} + \frac{1}{3} [2\omega_L^2(k) - (1/\tau_k)^2]. \quad (10)$$

A sufficient criterion for the presence of these peaks is given by the condition $3\langle \omega_k^2 \rangle \geq \omega_L^2(k)$, irrespective of the value of τ_k . The inequality is not satisfied for large k [where $\langle \omega_k^2 \rangle \rightarrow (k_B T/M)k^2$ and $\omega_L^2(k) \rightarrow 3(k_B T/M)k^2 + \Omega_0^2$], even if in this nearly free-particle regime the viscoelastic model is increasingly unable to reproduce the detailed shape of $S(k, \omega)$, which should eventually become a Gaussian centered at $\omega = 0$. On the other hand, for small wave vectors the criterion implies that $\frac{1}{10} S(0)\Gamma \leq 1$; thus, in systems with a larger value of Γ (e.g., with increasing Einstein frequencies), it becomes more and more difficult to observe well-defined peaks in $S(k, \omega)$. For example, liquid alkali metals (which have a relatively soft repulsive potential, i.e., a low Γ) are known to support well-defined density modes over a wave-vector range which is noticeably larger than in liquid argon, where the harsh, Lennard-Jones-like repulsion increases the value of Ω_0^2 and consequently of Γ . As a result, whereas a large value of the product $S(0)\Gamma$ makes the density modes virtually unobservable beyond the hydrodynamic regime, it increases the difference between the two velocities c_T and c_∞ .

In addition to $S(k, \omega)$, it is convenient to consider the spectrum associated with the longitudinal current correlation function, defined by $C_L(k, \omega) = \omega^2 S(k, \omega)$. Being zero at $\omega = 0$, $C_L(k, \omega)$ always has a maximum at finite frequencies; often, the physics behind this peak is “trivial” in the sense that no additional information beyond

the one directly evident from $S(k, \omega)$ can be gained. However, some otherwise undiscernible effects can in fact be detected from $C_L(k, \omega)$ in the k range where the inelastic peaks in $S(k, \omega)$ are ill defined. The prediction of the viscoelastic model for $C_L(k, \omega)$ reads

$$\frac{C_L(k, \omega)}{k^2 k_B T/M} = \frac{(1/\pi)\omega^2 \Delta_k (1/\tau_k)}{\omega^2 [\omega^2 - \omega_L^2(k)]^2 + (1/\tau_k)^2 [\omega^2 - \langle \omega_k^2 \rangle]^2}. \quad (11)$$

The peak frequencies $\omega_C(k)$ of $C_L(k, \omega)$ follow from the physical solutions of the following cubic equation in ω^2 :

$$2(\omega^2)^2 [\omega^2 - \omega_L^2(k)] + (1/\tau_k)^2 [(\omega^2)^2 - \langle \omega_k^2 \rangle^2] = 0. \quad (12)$$

Two limiting solutions of this equation are of particular interest. For very small wave vectors, noting that both $\omega_L^2(k)$ and $\langle \omega_k^2 \rangle$ vanish as k^2 whereas $(1/\tau_k)^2$ stays finite, Eq. (11) has the approximate solution $\omega_C^2(k) = \langle \omega_k^2 \rangle + O(k^4)$, namely, the result of ordinary (isothermal) hydrodynamics. On the other hand, at larger wave vectors (namely, higher frequencies) all the quantities in Eq. (12) are finite and one may exploit the fact that $\omega_L^2(k)$ is often distinctly larger than $\langle \omega_k^2 \rangle$, obtaining the simple analytic result

$$\omega_C^2(k) \approx \omega_L^2(k) - \frac{1}{2} (1/\tau_k)^2. \quad (13)$$

The validity of Eq. (13) worsens if $(1/\tau_k)$ becomes comparable with $\omega_L(k)$; slightly better approximations may be found in such a circumstance. In any case, as k increases there is always a clear tendency of the peak frequency of $C_L(k, \omega)$ to move from the hydrodynamic result $\langle \omega_k^2 \rangle^{1/2}$ upwards to a steeper dispersion law, which approaches $\omega_L(k)$ in the case of a relatively long relaxation time τ_k . As a matter of fact, if the frequencies under consideration are much larger than the relaxation rate $1/\tau_k$ the system responds with the frequency $\omega_L(k)$, and with the associated velocity $c_\infty(k) = \omega_L(k)/k$ — a typical “instantaneous” solidlike response. Consequently, as k increases the “sound velocity” $v_C(k) \equiv \omega_C(k)/k$ pertinent to the density current mode is intermediate between $c_T(k)$ and $c_\infty(k)$. The actual values of $v_C(k)$, as well as the wave-vector range where the transition occurs, depend on the efficiency of the relaxation process of $M(k, t)$, often referred to as “shear relaxation” [5] because of the aforementioned connection of the memory function with the onset of viscous effects.

There are several “recipes” to evaluate the time constant τ_k , based on interpolation procedures between the hydrodynamic value (9) and the free-particle situation which prevails at large wave vectors (see Ref. [6]). We shall not discuss these schemes, which often introduce additional assumptions and/or parameters which are difficult to justify *a priori*. Broadly speaking, one expects a substantial decrease of the time τ_k at increasing wave vectors, where the dynamics is explored at an increasingly microscopic level. An *empirical* determination of $1/\tau_k$ is readily obtained exploiting the fact that the line shape predicted by the viscoelastic model can be fitted rather successfully to the experimental or simulation data. This

is particularly true for all the liquid alkali metals, which in the present context are also interesting because they share with water a nearly isothermal hydrodynamic behavior. In the finite wave-vector region of interest for the “anomalous” sound, the relaxation rate in these simple liquids is indeed found to increase rather strongly from its hydrodynamic value $1/\tau_0$. This increase is approximately linear, a trend similar to the k dependence of $\omega_L(k)$ in the same wave-vector range; combining these two circumstances with Eq. (13) for $\omega_C(k)$, we easily see how a “soundlike” linear dispersion law may indeed be observed even at these nonhydrodynamic wave vectors.

To give an example of this situation in a specific case, we report in Fig. 1 the quantities $\langle \omega_k^2 \rangle$ and $\omega_L^2(k)$ as evaluated for liquid Cs near the melting point using our computer simulation data in this system [8]. Like all alkali metals, liquid Cs is characterized by a relatively soft potential; in the simulations a convenient modeling of $v(r)$ is provided by an effective pair potential implemented by Price, Singwi, and Tosi [9]. The softness of $v(r)$ and the large mass of Cs imply a small value of $\Omega_0^2 = 19.22 \text{ ps}^{-2}$ (to be compared, e.g., with $\Omega_0^2 = 59.3 \text{ ps}^{-2}$ found for Lennard-Jones liquid Ar). Like water, liquid alkali metals have a specific heat ratio $\gamma \approx 1$: for Cs ($\gamma = 1.1$), the isothermal sound velocity $c_T \approx 900 \text{ m/s}$ is not very different from the experimental value 965 m/s . At increasing wave vectors, the criterion for the propagation of well-defined “sound modes” is easily satisfied in liquid Cs, where $\frac{1}{10}S(0)\Gamma = 0.546 < 1$. As a matter of fact, recent neutron-scattering experiments [10] have reported the presence of inelastic peaks in $S(k, \omega)$ even at wave vectors as high as 1.2 \AA^{-1} . On the other hand, this situation implies that the ratio c_∞/c_T is not large [from Eq. (7), $c_\infty/c_T = 1.28$ for Cs, to be, e.g., compared with $c_\infty/c_T = 2.16$ for liquid Ar]. As a consequence, the values of the “velocity” $v_C(k)$ are not expected to be much higher than c_T . The observed increase of the “sound velocity” in liquid Cs is indeed found to be rather small, with a maximum magnitude of about 20% in the

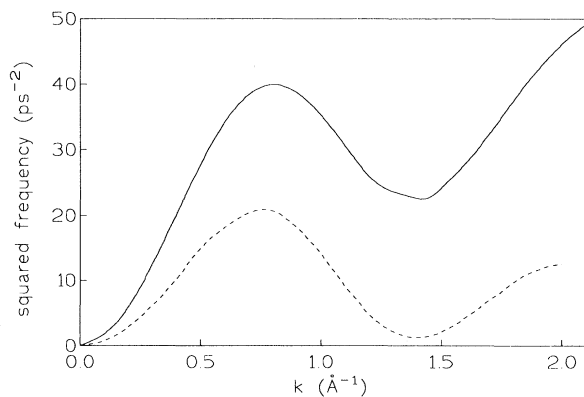


FIG. 1. The quantities $\langle \omega_k^2 \rangle$ (dashed line) and $\omega_L^2(k)$ (full line) in liquid Cs at $T = 308 \text{ K}$ and a number density $n = 0.0083 \text{ \AA}^{-3}$. The results have been deduced from the structural data obtained in the computer simulation experiment of Ref. [8].

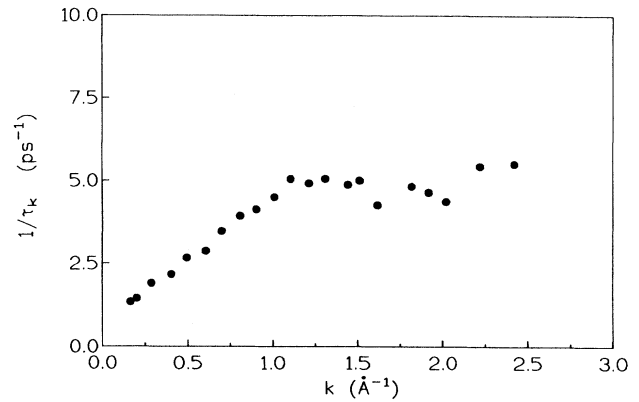


FIG. 2. The shear relaxation rate $1/\tau_k$ in liquid Cs as obtained by a fitting of the viscoelastic $S(k, \omega)$ to the spectral shapes observed at different wave vectors.

range $k \approx 0.35 \text{ \AA}^{-1}$ [10].

Our simulation data for $S(k, \omega)$ are found to agree with the neutron spectra over all the explored wave-vector range [8]. Moreover, the spectral shapes are satisfactorily reproduced by the viscoelastic model where the parameter $(1/\tau_k)$ is determined by a fitting procedure. The values deduced for $(1/\tau_k)$ are reported in Fig. 2; note that although for $k \approx 0.3\text{--}0.4 \text{ \AA}^{-1}$ the relaxation rate is substantially larger than $1/\tau_0 \approx 0.4 \text{ ps}^{-1}$, $(1/\tau_k)^2$ is still much smaller than $\omega_L^2(k)$ so that the velocity $v_C(k)$ deduced from Eq. (12) nearly coincides with $c_\infty(k) = \omega_L(k)/k$. The results for these k -dependent velocities are summarized in Fig. 3, which shows a good overall agreement between $v_C(k)$ and the simulation and/or the neutron data. The maximum $v_C(k)$ is $\approx 1150 \text{ m/s}$ near $k = 0.3 \text{ \AA}^{-1}$, where $c_\infty(k)$ is $\approx 1180 \text{ m/s}$.

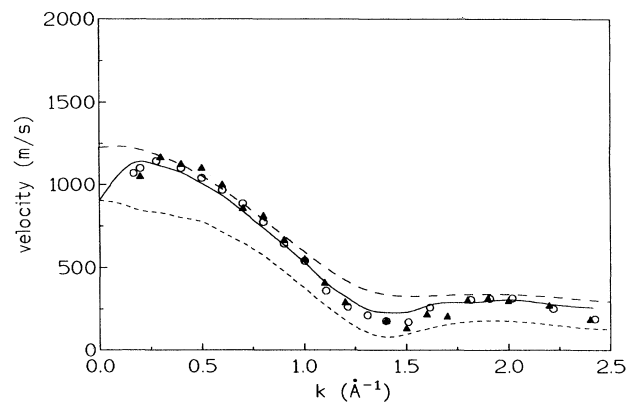


FIG. 3. Wave-vector dependence of the different “velocities” in liquid Cs. The dashed line is the k -dependent isothermal sound velocity $c_T(k) = \langle \omega_k^2 \rangle^{1/2}/k$. The long-dashed line is $c_\infty(k) = \omega_L(k)/k$, and the full line is $v_C(k) = \omega_C(k)/k$ with $\omega_C(k)$ obtained from Eq. (12). The data are the values of $v_C(k)$ deduced from the peaks of $C_L(k, \omega)$ as observed in the simulation of Ref. [8] (open circles) and in the real experiment of Ref. [10] (triangles).

III. COLLECTIVE DYNAMICS IN LIQUID WATER

We shall now discuss the consequences of a formally similar analysis when applied to the more intriguing case of liquid water. Most of the previous considerations can be repeated for a system made of rigid molecules, provided that we focus our attention on the molecular centers of mass. In water, the latter may be taken as approximately coincident with the positions of the oxygen atoms, since the small corrections (of the order m_H/M , where m_H is the hydrogen mass and M the molecular mass) are entirely negligible on the scale of the phenomenon to be explained (the huge "anomaly" in the sound propagation). Denoting by $\mathbf{r}_j^{(c)}(t)$ the position of the center of mass of the j th molecule at time t , one introduces an intermediate scattering function for the centers of mass

$$F^{(c)}(\mathbf{k}, t) = (1/N) \sum_{i,j} \langle \exp\{-i\mathbf{k} \cdot [\mathbf{r}_i^{(c)}(0) - \mathbf{r}_j^{(c)}(t)]\} \rangle - 8\pi^3 n \delta(\mathbf{k}), \quad (14)$$

with initial value $F^{(c)}(\mathbf{k}, 0) = S^{(c)}(\mathbf{k}) \approx S_{OO}(\mathbf{k})$, the oxygen partial structure factor. The dynamics of $F^{(c)}(\mathbf{k}, t)$ at very short times is again ruled by the quantity $\langle \omega_k^2 \rangle^{(c)} = [k_B T / MS^{(c)}(\mathbf{k})] k^2$. In analogy with the previous treatment for monatomic systems, we introduce the quantity $\omega_L^2(k)$ which is directly affected by the intermolecular potential. Writing the latter in terms of pairwise contributions $v(\mathbf{r}_1^{(c)} - \mathbf{r}_2^{(c)}; \Omega_1, \Omega_2)$, $\omega_L^2(k)$ can again be formally written as in Eq. (2) with the quantity Ω_k^2 defined by

$$\Omega_k^2 = (n/M) \int d\mathbf{r}^{(c)} \exp(ikz^{(c)}) \times \left\langle \frac{\partial^2 v(\mathbf{r}^{(c)}; \Omega_1, \Omega_2)}{\partial z^{(c)2}} g(\mathbf{r}^{(c)}; \Omega_1, \Omega_2) \right\rangle_{\Omega}, \quad (15)$$

where $\mathbf{r}^{(c)} = \mathbf{r}_1^{(c)} - \mathbf{r}_2^{(c)}$, and $\langle \rangle_{\Omega}$ denotes an average over the molecular orientations Ω_1 and Ω_2 . Equation (15) can be simplified if the potential is written in terms of site-site contributions

$$\omega_L^2(k) = 3[k_B T / M] k^2 + (1/M) \{ [A_{OO}^{LJ}(0) - A_{OO}^{LJ}(k)] + [4A_{HH}^C(0) + 4A_{OH}^C(0) + A_{OO}^C(0)] - [4A_{HH}^C(k) + 4A_{OH}^C(k) + A_{OO}^C(k)] \}. \quad (20)$$

This result can be simplified for the Coulombic part, which involves the potential $v_{\alpha\beta}^C(r) = q_{\alpha} q_{\beta} / r$ where q_{α} and q_{β} are effective charges. Using the definition (16) of $A_{\alpha\beta}(0)$, it is readily found that the quantity $[4A_{HH}^C(0) + 4A_{OH}^C(0) + A_{OO}^C(0)]$ is proportional to $(2q_H + q_O)^2 \equiv 0$ because of the electrical neutrality of the molecule. Finally, for the explicit evaluation of $\omega_L^2(k)$ it is convenient to extract any dimensional quantity by defining $A_{OO}^{LJ}(k) \equiv 4\pi(\epsilon/3\sigma^2)n\sigma^3 a_{OO}^{LJ}(k)$ and $A_{\alpha\beta}^C(k) \equiv 8\pi n Z_{\alpha} Z_{\beta} e^2 a_{\alpha\beta}^C(k)$, where ϵ and σ are the usual Lennard-Jones parameters for the oxygen atoms and $q_{\alpha,\beta} = Z_{\alpha,\beta} |e|$ with $Z_O = -2Z_H$. In such a way we find

$$v(\mathbf{r}^{(c)}; \Omega_1, \Omega_2) = \sum_{\alpha,\beta} v_{\alpha\beta}(r_{1\alpha,2\beta}), \quad (16)$$

where the summation runs over all the interaction sites considered over the molecule. In such a case the analog of the Einstein frequency for the molecular system can be written as

$$\Omega_0^2 = (4\pi n / 3M) \sum_{\alpha,\beta} \int_0^{\infty} dr r^2 \{ v''_{\alpha\beta}(r) + 2[v'_{\alpha\beta}(r)/r] \} \times g_{\alpha\beta}(r) \equiv (1/M) \sum_{\alpha,\beta} A_{\alpha\beta}(0), \quad (17)$$

where $g_{\alpha\beta}(r)$ are the site-site pair distribution functions. At finite (yet relatively small) wave vectors, one may approximately write Ω_k^2 in a form similar to Eq. (3), namely,

$$\Omega_k^2 \approx (n/M) \sum_{\alpha,\beta} \int d\mathbf{r} \exp(ikz) \frac{\partial^2 v_{\alpha\beta}(r)}{\partial z^2} g_{\alpha\beta}(r) \equiv (1/M) \sum_{\alpha,\beta} A_{\alpha\beta}(k). \quad (18)$$

As a result

$$\omega_L^2(k) = 3[k_B T / M] k^2 + (1/M) \sum_{\alpha,\beta} [A_{\alpha\beta}(0) - A_{\alpha\beta}(k)]. \quad (19)$$

To evaluate the quantities $A_{\alpha\beta}(k)$ we need a model for the site-site potentials $v_{\alpha\beta}(r)$. In the case of water, the simplest model is provided by the three-site simple point charge (SPC) potential [11], in which the sites coincide with the positions of the atoms in the H_2O molecule. The more refined four-site TIP4P potential [12] is found to yield nearly the same results for the partial structure factors $S_{\alpha\beta}(k)$, the slight differences being due to the small distance of the additional site from the oxygen atom (or from the molecular center of mass). The quantities $A_{\alpha\beta}(k)$ are conveniently split into Coulombic (C) and Lennard-Jones (LJ) intermolecular contributions, the latter being only associated with the oxygen-oxygen interactions. Then

$$\omega_L^2(k) = 3[k_B T / M] k^2 + (4\pi/M) \{ (\epsilon/3\sigma^2) n \sigma^3 [a_{OO}^{LJ}(0) - a_{OO}^{LJ}(k)] - 8\pi n Z_{He}^2 [a_{HH}^C(k) - 2a_{OH}^C(k) + a_{OO}^C(k)] \}. \quad (21)$$

The result (21) has been numerically evaluated in the TIP4P case by using the pair distribution functions $g_{\alpha\beta}(r)$ provided by the computer simulations of Frattini *et al.* [13] which satisfactorily account for the observed structural properties of water at room temperature. The values obtained in this way for $\omega_L^2(k)$ are reported in Fig.

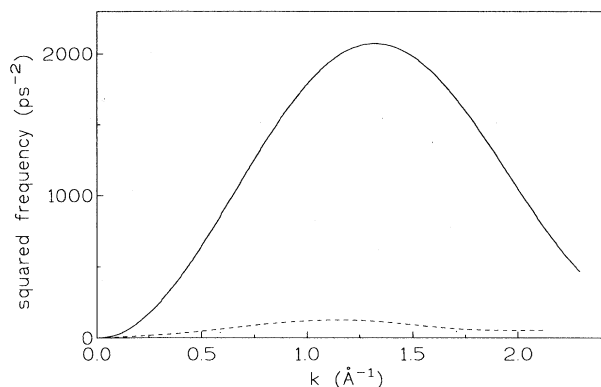


FIG. 4. The quantities $\langle \omega_k^2 \rangle^{(c)}$ (dashed line) and $\omega_L^2(k)$ (full line) for water at $T \approx 310$ K (number density $n = 0.0333 \text{ \AA}^{-3}$).

4 together with those for the quantity $\langle \omega_k^2 \rangle^{(c)}$.

Comparing with the corresponding results for liquid Cs (Fig. 1), the difference between $\omega_L^2(k)$ and $\langle \omega_k^2 \rangle^{(c)}$ appears to be much larger in the case of water. The effect is essentially due to a quite dramatic increase of $\omega_L^2(k)$ with respect to the liquid metal through all the explored wave-vector range. In turn, this increase is largely due to the much higher Einstein frequency in H_2O : from Eq. (18) it is found that $\Omega_0^2 \approx 1210 \text{ ps}^{-2}$, almost 65 times the value obtained for liquid Cs. Although this huge difference is partly due to "trivial" factors like the smaller values of the mass M and the length σ , an important contribution is also provided by the intermolecular repulsion, which is considerably harder in water than in the liquid metal. An unambiguous measure of this feature is provided by the dimensionless parameter $\Gamma = M\Omega_0^2\sigma^2/k_B T$, which is still four times larger in water ($\Gamma \approx 850$) than in liquid Cs ($\Gamma \approx 220$). In this respect, liquid Ar with $\Gamma \approx 385$ appears to be an intermediate case, which will be discussed in detail in the following section.

For our purposes, another noteworthy difference between the two limiting cases of water and the liquid metal concerns the isothermal compressibility, proportional to the $k=0$ value of the structure factor $S(k)$. Whereas $S(0) \approx 0.023$ for all the liquid alkali metals near the melting point, $S(0) \approx 0.065$ for water at room temperature. In this case the physical origin of the difference is more subtle than for Ω_0^2 , since $S(0)$ depends on the character of the intermolecular potential at large distances [an average attractive tail leading to a larger value of $S(0)$, and vice versa]. In contrast with water, liquid metals are known to have an oscillatory potential at large r , thus making their $S(0)$ not very different from the hard-sphere value (≈ 0.018 at comparable densities).

IV. DISCUSSION AND CONCLUDING REMARKS

Having in mind the considerations previously discussed for the monatomic liquid, it is now straightforward to make the following "predictions" for the features

to be expected for the dynamics of the centers of mass in H_2O .

(i) First of all, in water the quantity $\frac{1}{10}S(0)\Gamma$ is ≈ 5.5 , making virtually impossible the observation of inelastic peaks (or well-defined density modes) in $S(k, \omega)$ outside the hydrodynamic regime. Indeed, no clear evidence of these peaks is provided by both inelastic neutron scattering [1] and simulation experiments [4] even at the smallest wave vectors which have been probed by these techniques (a few tenths of \AA^{-1}). This situation is qualitatively analogous to the one found for liquid Ar near the triple point, for which the quantity $\frac{1}{10}S(0)\Gamma \approx 1.56$, albeit much smaller than in H_2O , is considerably larger than 1 [14].

(ii) The subtle aspects of the dynamics in this wave-vector range are more apparent if one considers the longitudinal current spectrum $C_L(k, \omega)$, as indeed is done in most simulation work (and indirectly even in the analysis of the neutron data in Ref. [1]).

(iii) As discussed previously, the ill-defined nature of density modes at finity k has as a counterpart a large value of the ratio $(c_\infty/c_T)^2$. As a matter of fact, in water the aforementioned numerical results yield $c_T \approx 1450$ m/s, $c_\infty \approx 5000$ m/s, and $c_\infty/c_T \approx 3.45$. The latter result is substantially larger than the values 1.28 for liquid Cs and 2.16 for liquid Ar.

(iv) As in the case of liquid Cs, the peak frequency $\omega_C(k)$ of $C_L(k, \omega)$ can exhibit even in water a linear dispersion outside the proper hydrodynamic regime, with a velocity $v_C(k) = \omega_C(k)/k$. The latter is likely to be considerably higher than c_T , in view of the large value of c_∞ . The actual magnitude of $v_C(k)$ depends on the efficiency of shear relaxation processes, as measured by $1/\tau_k$. This decay rate can in principle be determined by a fitting procedure analogous to the one previously adopted for liquid Cs, even if the relatively few wave vectors explored in the available data prevent an accurate determination of the k dependence. In any case, $1/\tau_k$ is found to be $\approx 26 \text{ ps}^{-1}$ in the wave-vector range where the anomalous dispersion was reported. Such a short relaxation time is of the same order of $1/\Omega_0$, namely, of the initial decay time of the velocity autocorrelation function for the molecular centers of mass. On the basis of the approximate result (13), $\omega_C^2(k)$ can now be expected to be noticeably smaller than $\omega_L^2(k)$; indeed, for $k = 0.425 \text{ \AA}^{-1}$ [where $\omega_L^2(k) \approx 484 \text{ ps}^{-2}$] the exact solution of Eq. (12) yields $\omega_C^2(k) \approx 153 \text{ ps}^{-2}$, which is still much larger than $\langle \omega_k^2 \rangle^{(c)} \approx 37 \text{ ps}^{-2}$. As a result, at these wave vectors the effective velocity $v_C(k)$ can be much higher than its hydrodynamic value $c_T \approx 1450$ m/s; in particular, for $k = 0.425 \text{ \AA}^{-1}$ one finds $v_C \approx 2915$ m/s, in good agreement with the value ≈ 3000 m/s deduced from the data of Ref. [1]. The overall situation encompassing the available data is summarized in Fig. 5, which is to be compared with the previous results reported for the liquid metal (Fig. 3). In water, the preliminary results of a simulation which we performed with a larger system (500 molecules) appear to indicate a substantial decrease of $v_C(k)$ at smallest wave vectors $k \approx 0.25 \text{ \AA}^{-1}$; this trend is expected, but all the spectral features in this interesting transition region need to be explored with a considerably higher accuracy than the one

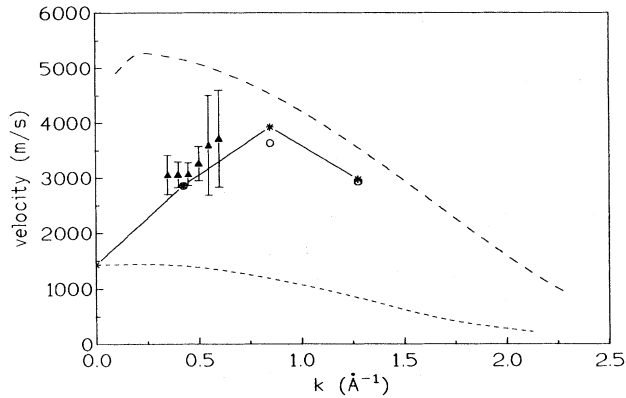


FIG. 5. Wave-vector dependence of the different “velocities” in liquid water at room temperature. The dashed lines have the same meaning as in Fig. 3. The asterisks denote the theoretical values of $v_c(k)$ with the relaxation rates deduced from a fitting procedure to the $F(k, t)$ data of Ref. [4]; the full straight lines are a guide for the eye. Symbols: neutron data from Ref. [1] (triangles) and values deduced from the peaks of $C_L(k, \omega)$ in the simulation of Ref. [4] (open circles).

of our present data. In this respect, the availability of new neutron data at wave vectors smaller than the ones explored in Ref. [1] would also be quite useful.

In conclusion, the peculiar dispersion law of liquid water stems from an unusually high value of $\omega_L^2(k)$ in the wave-vector region where the fast sound has been observed. In terms of site-site potentials, throughout this k range $\omega_L^2(k)$ is essentially determined by the oxygen-oxygen intermolecular interaction, approximated by a Lennard-Jones potential both in the SPC and in the TIP4P potential models. In turn, for these wave vectors the magnitude of $\omega_L^2(k)$ is controlled by the huge values of the squared Einstein frequency

$$\Omega_0^2 = (1/M) A_{OO}^{LJ}(0) \equiv (4\pi/3)(\epsilon/M\sigma^2)n\sigma^3 a_{OO}^{LJ}(0). \quad (22)$$

As already remarked, the harsh repulsive part of the LJ potential provides an important contribution in the increase of the Einstein frequency in water (or even in argon) with respect to liquid Cs. However, this factor alone would not be sufficient to justify the high value of the quantity $a_{OO}^{LJ}(0)$ in water. For example, Ω_0^2 in H_2O is a factor ≈ 20 larger than the corresponding quantity in LJ Ar; taking into account the “trivial” dimensional factor $(\epsilon/M\sigma^2)n\sigma^3$ we are still left with a ratio ≈ 10 between the dimensionless “Einstein frequencies” $a^{LJ}(0)$ in the two systems (≈ 770 in water and 81.2 in liquid Ar). This difference cannot be accounted for by the potential shape, the latter being the same in both cases.

The solution lies in the different ranges of separations effectively relevant in the two systems. In a simple monatomic liquid like Ar or Cs [Fig. 6(a)] the pair distribution function $g(r)$ has a main peak at a separation R which is slightly larger than σ and more or less coincident with the position of the first minimum of $v(r)$. In such a case,

the Einstein frequency probes the derivatives of $v(r)$ evaluated at separations $r \approx R \approx \sigma$.

In contrast, in H_2O the principal peak of the oxygen-oxygen pair distribution function is located at a distance considerably shorter than the Lennard-Jones $\sigma \approx 3.15$ Å appropriate for the oxygen atoms [see Fig. 6(b)] [15]. This circumstance is due to the influence on $g_{OO}(r)$ of the intermolecular interactions other than the “direct” LJ one. In particular, in the previous potential models the effect is due to the electrostatic interactions, whose magnitude is chosen in such a way that the simulation reproduces several structural features typical of liquid water, as the tetrahedral arrangement around a molecule and the collinear O—H—O bond. As a result, the position of the main peak of $g_{OO}(r)$ is now such that Ω_0^2 effectively probes the derivatives of $v_{OO}^{LJ}(r)$ for separations distinctly smaller than σ , i.e., in a range where the LJ potential is very steep. The consequent high value of the derivatives leads to the “unusually” large Einstein frequency, and ultimately to the striking magnitude of the anomalous dispersion in liquid water.

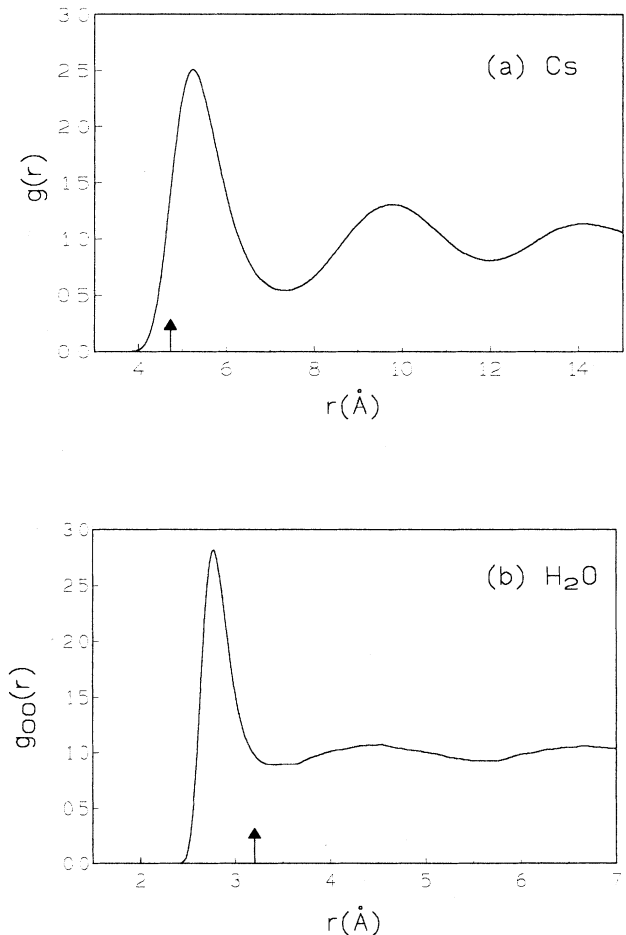


FIG. 6. Simulation data for the pair distribution functions: (a) $g(r)$ in liquid Cs at 308 K (Ref. [8]); (b) $g_{OO}(r)$ in water at 310 K (Ref. [13]). The arrows indicate the values of σ in the two systems.

As a final evidence of the correctness of these arguments, let us consider another molecular liquid, namely, H_2S . In this case the molecular geometry is known to be rather similar to the one of water. Moreover, for H_2S Forester, McDonald, and Klein [16] have proposed a convenient site-site potential model whose form is apparently analogous to the TIP4P model for water: electrostatic interactions among four charged sites, plus a LJ interaction between the sulfur atoms. This intermolecular potential was adopted in the computer experiment of Ref. [13] to simulate H_2S at a temperature $T \approx 208$ K. The data of the velocity autocorrelation function for the centers of mass indicate that in this case the Einstein frequency is $\Omega_0^2 \approx 158 \text{ ps}^{-2}$, much smaller than in water. Extracting the dimensional factor $(\epsilon/M\sigma^2)n\sigma^3$, we deduce that the quantity $a^{\text{LJ}}(0)$ is now 89.4, a figure noticeably smaller than $a^{\text{LJ}}(0) \approx 770$ for water but entirely consistent with the value 81.2 found for liquid argon. Since in all three systems the relevant interaction directly entering Ω_0^2 is the Lennard-Jones potential, these differences must be due to the pair distribution functions. Indeed, it is found [13,16] that in H_2S the overall features of $g_{\text{SS}}(r)$ are remarkably similar to those of a monatomic liquid. In particular, the molecules are close packed (average coordination number ≈ 12) and the main peak is located at a distance slightly larger than the sulfur σ .

These results are in marked contrast with the situation found for water, and explain the much lower values found for A and Ω_0^2 in H_2S . Pursuing all the previous arguments, it is now straightforward to predict that any "anomalous" dispersion effect should be considerably smaller in H_2S than in H_2O . This is indeed what is found in a recent simulation work [17], which for the effective sound velocity $v_C(k)$ reports an increase of $\approx 40\%$ with respect to the isothermal speed of sound $c_T \approx 1170$ m/s, to be compared with the corresponding $\approx 100\%$ increase found for water.

ACKNOWLEDGMENTS

The authors wish to thank Chr. Morkel for providing an extensive account of the neutron-scattering data in liquid Cs. This work has partially been supported by the European Economic Community under Contract No. SC1-CT91-0714 (TSTS). For our simulations, we gratefully acknowledge the cooperation of CINECA (Centro di calcolo elettronico interuniversitario dell'Italia nord-orientale) for Grant No. G9LTNZM1 (1992). Part of the computing time was made available under a convention between CINECA and CNR (Consiglio Nazionale delle Ricerche).

-
- [1] J. Teixeira, M. C. Bellissent-Funel, S. H. Chen, and B. Dorner, *Phys. Rev. Lett.* **54**, 2681 (1985).
- [2] A. Rahman and F. H. Stillinger, *Phys. Rev. A* **10**, 368 (1974).
- [3] M. Wojcik and E. Clementi, *J. Chem. Phys.* **85**, 6085 (1986).
- [4] M. A. Ricci, D. Rocca, G. Ruocco, and R. Vallauri, *Phys. Rev. A* **40**, 7226 (1989).
- [5] J. P. Boon and S. Yip, *Molecular Hydrodynamics* (McGraw-Hill, New York, 1980).
- [6] J. R. Copley and S. W. Lovesey, *Rep. Prog. Phys.* **38**, 461 (1975).
- [7] J. W. Lewis and S. W. Lovesey, *J. Phys. C* **10**, 3221 (1977).
- [8] U. Balucani, A. Torcini, and R. Vallauri, *Phys. Rev. A* **46**, 2159 (1992).
- [9] D. L. Price, K. S. Singwi, and M. P. Tosi, *Phys. Rev. B* **2**, 2983 (1970).
- [10] T. Bodensteiner, Chr. Morkel, P. Müller, and W. Gläser, *J. Non-Cryst. Solids* **117-118**, 941 (1990); T. Bodensteiner, Chr. Morkel, W. Gläser, and B. Dorner, *Phys. Rev. A* **45**, 5709 (1992).
- [11] H. J. Berendsen, J. P. M. Postma, W. F. van Gunsteren, and J. Hermans, in *Intermolecular Forces*, edited by B. Pullman (Reidel, Dordrecht, 1981), p. 331.
- [12] W. J. Jorgensen, J. Chandrasekhar, J. D. Madura, R. W. Impey, and M. L. Klein, *J. Chem. Phys.* **79**, 926 (1983).
- [13] R. Frattini, M. A. Ricci, G. Ruocco, and M. Sampoli, *J. Chem. Phys.* **92**, 2540 (1990). For the TIP4P potential parameters relevant for Eq. (21), this work reports $\epsilon = 1.077 \times 10^{-14}$ erg, $\sigma = 3.154 \text{ \AA}$, and $Z_H = 0.52$.
- [14] It is worthwhile to note that the viscoelastic criterion $\frac{1}{10}S(0)\Gamma \leq 1$ for the appearance of inelastic peaks in $S(k, \omega)$ is not to be taken too literally in liquid argon, which has a specific heat ratio $\gamma \approx 2$ and consequently a low- k dynamics far from isothermal. In any case, the minimum wave vector explored experimentally in this system near freezing was $k \approx 1 \text{ \AA}^{-1}$, too high to see any inelastic peak [K. Sköld, J. M. Rowe, G. Ostrowski, and P. D. Randolph, *Phys. Rev. A* **6**, 1107 (1972)]. On the other hand, a remnant of a Brillouin peak is apparent only up to $k\sigma \approx 1$ ($k \approx 0.3 \text{ \AA}^{-1}$ in Ar) in the simulation data for Lennard-Jones systems near the triple point [D. Levesque, L. Verlet, and J. Kärkkjärvi, *Phys. Rev. A* **7**, 1690 (1973)].
- [15] Strictly speaking, this circumstance decreases somewhat the validity of the approximation $R \approx \sigma$ in the right-hand side of Eq. (4) when applied to water. In fact, the numerical results for $\omega_L^2(k)$ are much better reproduced by Eq. (4) taking $R = 0.89\sigma$, i.e., a value very near the position of the main peak of $g_{\text{OO}}(r)$. As a result, for water the parameter Γ is effectively decreased by $\approx 20\%$ to $\Gamma \approx 680$, making less dramatic the difference with liquid argon ($\Gamma \approx 385$).
- [16] T. R. Forester, I. R. McDonald, and M. L. Klein, *Chem. Phys.* **129**, 225 (1989).
- [17] M. A. Ricci, G. Ruocco, D. Rocca, and R. Vallauri, *J. Chem. Phys.* **93**, 9012 (1990).